

Open three-dimensionally ordered macroporous composite Ag/TiO₂: synthesis and multi-modes photocatalytic degradation Malachite green

Shuhua Li^{a,†}, Yuting Hao^{b,†}, Yiwen Zhu^{a,b}, Li Li^{a,b,*}

^aCollege of Materials Science and Engineering, Qiqihar University, Qiqihar 161006, China, Tel. +86 0452-2738867; email: qqhrll@163.com/qqhrlili@126.com

^bCollege of Chemistry and Chemical Engineering, Qiqihar University, Qiqihar 161006, China

Received 17 March 2021; Accepted 27 June 2021

ABSTRACT

The three-dimensionally ordered macroporous composite Ag/TiO₂ was synthesized by vacuum filtration and the calcined treatment. X-ray diffraction, X-ray photoelectron spectroscopy, UV-Vis diffuse reflectance spectroscopy, scanning electron microscopy, and N₂ adsorption–desorption measurements were employed to characterize its composition, structure, morphology, and surface physicochemical properties. The results showed that as-composite had good crystal structure, of which connected holes were neat, orderly, open and transparent, which belonged to three-dimensionally ordered macroporous materials (3DOM). Moreover, with polystyrene colloidal crystal as the template, the surface area of 3DOM Ag/TiO₂ composite significantly increased. During the degradation of Malachite green under multi-modes photocatalytic experiments, including the ultraviolet, visible and simulated sunlight irradiation, the 3DOM Ag/TiO₂ composite exhibited better photocatalytic activity than that of Ag/TiO₂ and TiO₂. Meanwhile, it also showed degradation effects on different pollutants. In addition, according to the trapping experiments under UV light irradiation, the possible photocatalytic reaction mechanism of 3DOM Ag/TiO₂ was proposed.

Keywords: Polystyrene; Three-dimensionally ordered macroporous materials; Ag/TiO₂; Multi-modes photocatalysis

1. Introduction

Currently, photocatalytic degradation as a kind of new energy-saving technology has widely attracted some researcher's attention. Titanium dioxide (TiO₂), owing to high photocatalytic activity, low cost, and other non-toxic and stability properties, has been considered as one of the very promising semiconductor materials [1]. However, wide band gap, photogenerated electrons and holes more likely compounding and other defects, have restricted the practical application of TiO₂ in the photocatalysis field to a certain extent. In order to enhance the catalytic activity of TiO₂, a variety of different synthetic methods have gradually been adopted, such as noble metal supporting,

ion doping, and semiconductor combining and so on. Wherein, the noble metal doped and the morphology optimized have become the hot spot [2–4]. During the past decade years, due to unique physicochemical properties and potential applications, metal nanoparticles have attracted people's attention [5]. Modifying TiO₂ nanoparticles by Au, Ag and Pt can improve the separation of photo-generated charge carrier, extend the photo-response region, thus increase its photocatalytic properties. Due to the relatively inexpensive Ag and its anti-virus effect, thus Ag has become one of the most widely used precious metals.

Since the photocatalytic activity of titanium dioxide is largely affected by the structure and morphology, some forms of titanium dioxide such as nanorods, nanotubes,

* Corresponding author.

[†]These authors contributed equally to this work and should be considered co-first authors.

hollow balls and other more structures have been studied [6]. In recent years, some studies about enhancing material performances by improving their morphologies are gradually increasing [7–9]. Among them, due to the macroporous structure and big specific area of three-dimensionally ordered macroporous materials (3DOM), the study of 3DOM has become more sophisticated, of which the synthesis method is mainly the colloidal crystal template method that was carried out by self-assembly manner of the microspheres template [10]. These materials with 3DOM structure usually have open pore structures, which is large pore net structure, in a periodic arrangement. Its openness can effectively reduce the mass transfer resistance, so it is very beneficial to the input and output of reactants and products in the catalytic process [11].

Accordingly, polystyrene (PS) colloidal spheres and triblock copolymer surfactant $\text{EO}_{20}\text{PO}_{70}\text{EO}_{20}$ (P123) were used as macroporous and mesoporous template to prepare 3DOM Ag/TiO_2 composite through the vacuum filtration and the calcined treatment. The purpose of this study: first, three-dimensionally ordered macroporous materials with regular and ordered arrangement are built under the action of dual templates; second, utilize the attraction effect of silver on the electron to reduce the recombination ratio of photogenerated electrons and holes in the process of photocatalytic reaction, and improve the photocatalytic activity of the composite material. At the same time, the doping of metal silver also can make spectral response range broaden to the visible region; thereby the light utilization of composite materials is improved. Malachite green was used as a model molecule in the experiment; the photocatalytic activities of 3DOM Ag/TiO_2 were investigated under ultraviolet, visible and simulated sunlight conditions, which also were compared with other systems, such as direct photocatalysis, Ag/TiO_2 and TiO_2 . Simultaneously, the photocatalytic reaction mechanism and the universality of 3DOM Ag/TiO_2 for pollutants degradation were also studied systematically.

2. Experimental

2.1. Materials

Titanium isopropoxide (TTIP, 98% purity) was purchased from New Jersey Company in American; $\text{EO}_{20}\text{PO}_{70}\text{EO}_{20}$ (P123, MW5560-5890) was purchased from Aldrich Company; styrene was purchased from Tianjin Chemical Reagent Co., Ltd., (China). Tianli; $\text{K}_2\text{S}_2\text{O}_8$ and AgNO_3 were

purchased from Tianjin Guangfu Fine Chemical Research Institute (China); Malachite green (MG), Congo red (CR), Methylene blue (MB), Crystal violet (CV) and salicylic acid (SA) (structural formula shown in Fig. 1) are commercially available analytical grade and used without further purification. Water used in all experiments was deionized.

2.2. Preparation of Ag/TiO_2 composite

Added 0.2 g P123 in isopropanol, under stirring added TTIP, followed by the addition of silver nitrate solution, wherein the molar ratio of Ti and Ag is 50:1, and continue stirring to form Ag/TiO_2 gel. Obtaining the sample at 200°C by temperature program hydrothermal treatment 2 h, after drying and calcining in 500°C for 7 h, the resulting composite material was labeled as Ag/TiO_2 . Under the same conditions, the product without Ag nitrate solution added was labeled as TiO_2 .

2.3. Preparation of 3DOM Ag/TiO_2 composite

Monodisperse PS colloidal spheres were synthesized by emulsifier-free emulsion synthesis [12,13]. 0.2 g P123 was added to isopropyl alcohol and stirred until completely dissolved then dropping TTIP, followed by adding AgNO_3 solution to form Ag/TiO_2 sol, wherein the molar ratio of Ti and Ag is 50:1. Then a certain amount of PS template was added into Ag/TiO_2 sol, suction filtration after stirring for some time, drying and calcining in 500°C for 7 h, and the resulting composite material was labeled as 3DOM Ag/TiO_2 .

2.4. Characterization

The phase and composition of the as-prepared samples were detected by Bruker AXS (D8) X-ray diffractometer (XRD) studies using an X-ray diffractometer with $\text{Cu K}\alpha$ as X-ray radiation under 60 kV and 80 mA and with the 2θ ranging from 20° to 80°. X-ray photoelectron spectroscopy (XPS) was performed using an ESCALAB 250Xi spectrometer equipped with $\text{Al K}\alpha$ radiation at 300 W. Scanning electron microscopy (SEM) analysis of the samples was determined by the Japanese Hitachi S-4700 scanning electron microscope, the working voltage of 5 kV. The specific surface area and pore size of the sample were measured by a Brunauer–Emmett–Teller (BET) specific surface area instrument (BeiShiDe Instrument Technology (Beijing) Co., Ltd., Model 3H-2000PS2) with nitrogen

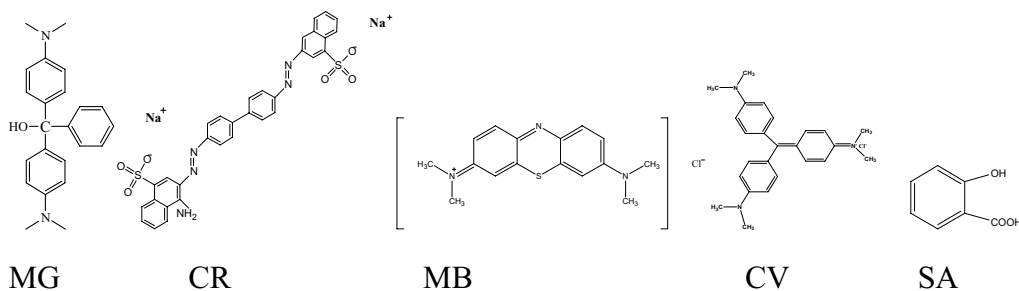


Fig. 1. The formula of different reactants.

adsorption at 77 K. The UV-Vis absorption spectra were recorded on a UV-Vis spectrophotometer (Model TU-1901) in the wavelength range of 200–800 nm, and BaSO_4 was used as the reference. The absorbance of the sample solution was determined by Beijing Purkinje General Company's TU-1901 UV-Visible double beam spectrophotometer.

2.5. Photocatalytic activity test

The photocatalytic activities of 3DOM Ag/TiO_2 composite were evaluated by photocatalytic degradation of Malachite green under multi-modes including UV, visible light, and simulated solar light irradiation. The experimental reaction devices of multi-mode light catalytic reaction are homemade, and the UV light source is 125 W high-pressure mercury lamp (built-in type, the maximum emission at 313.2 nm); the visible light was obtained from a 400 W Xe lamp (built-in type, the main emission lines greater than 410 nm; the inner sleeve was made of No. 11 glass to filter out ultraviolet from the Xe lamp). A simulated sunlight source was carried out by using a 1,000 W Xe-lamp (external type, Shanghai Bilon Instruments Co., Ltd.; the emission spectrum is close to the full spectrum). MG was used as a model dye. Moreover, the reaction liquid volumes of the three modes were 90, 220, and 90 mL, and the dosages of the catalyst were 0.15, 0.30 and 0.15 g, the degradation time of the three modes were 120, 180, and 300 min, respectively.

Process of photocatalytic reaction: prior to irradiation, a certain amount of photocatalyst was suspended in 90, 220 or 90 mL of MG (50 mg L^{-1}) solution by ultrasound ca.10 min, and then the suspensions were magnetically stirred for 30 min in the dark to ensure the adsorption-desorption equilibrium between MG and photocatalyst powders. The photocatalytic experiment was carried out in the photocatalytic reaction device. The catalysts were removed by centrifugation after the completion of the reaction. First, the experimental device was carried out under UV radiation as follows: the high-pressure mercury lamp was placed into a jacketed quartz tube. The quartz tube was soaked into the solution which was continuously magnetically stirred, and the suspensions were kept at constant temperature by circulating water through the jacket during the entire process. Second, the installation of the visible light degradation Malachite green was in accord with UV radiation except for lamp source. Third, during the process of the simulated solar light irradiation, MG solution and photocatalyst were taken in a quartz photo-reactor. The reactor was placed 8.5 cm away from the light source. The suspensions were kept at room temperature by circulating thermostatic ethanol through the jacket. Then, the absorption spectrum of the centrifugated solution was recorded using a TU-1901 UV-Vis spectrophotometer (China). The change of MG concentration was determined by monitoring the optical intensity of absorption spectra at 618 nm.

To infer the photocatalytic oxidation pathways of 3DOM Ag/TiO_2 , EDTA-2Na (10 mM), BQ (1 mM) and TBA (10 mM) were selected as scavenger agents for holes (h^+), oxygen radical anion ($\cdot\text{O}_2^-$) and hydroxyl radicals ($\cdot\text{OH}$), respectively, for the photocatalytic degradation of MG over

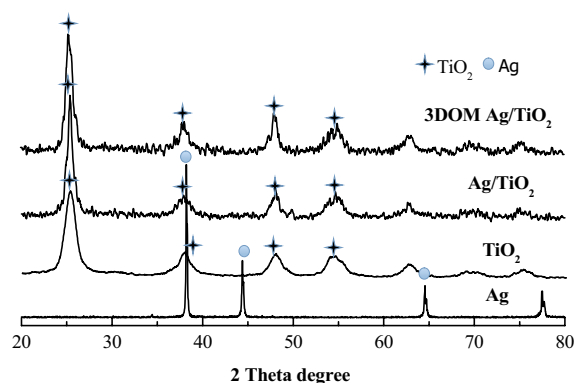


Fig. 2. XRD patterns of Ag, TiO_2 , Ag/TiO_2 and 3DOM Ag/TiO_2 .

3DOM Ag/TiO_2 composite. The determination of the concentration of MG during the photocatalytic reaction in the presence of EDTA-2Na, BQ or TBA was also determined by measuring the absorption of MG solution at 618 nm.

3. Results and discussion

3.1. X-ray diffraction

In order to examine the crystal structure of 3DOM Ag/TiO_2 composite, X-ray diffraction analysis was used to characterize and compare with Ag, TiO_2 and Ag/TiO_2 samples, the results shown in Fig. 2. As it can be seen from Fig. 2, pure Ag corresponding to cubic crystalline phase (JCPDS 03-0921), and the diffraction peaks of Ag/TiO_2 and 3DOM Ag/TiO_2 synthesized are consistent with the characteristic diffraction peaks of TiO_2 anatase phase (JCPDS 21-1272) [14]. It showed that the crystalline of as-composites is mainly based on anatase TiO_2 after silver doped. In addition, the characteristic diffraction peaks of silver had not been seen in the XRD spectra of as-composites, it may be attributed to the low content of the silver in the process of synthesis or the silver highly dispersed on the surface of titanium dioxide in the form of micro-crystals [15]. In order to investigate the influence of Ag on the TiO_2 lattice of different composites, the unit cell parameters of each composite were calculated (Table 1). Table 1 showed the unit cell parameters of 3DOM Ag/TiO_2 and Ag/TiO_2 were basically the same as pure TiO_2 , indicating that silver doping did not have an impact on the TiO_2 lattice, which was dispersed on the TiO_2 crystalline phase surface in the form of microcrystalline. The grain size calculated by the Scherrer equation of each as-sample can be seen in Table 1, compared with TiO_2 monomer, the grain sizes of 3DOM Ag/TiO_2 and Ag/TiO_2 composite was almost no change; indicating that silver doping had not more impact on the TiO_2 crystal form and crystallinity.

3.2. X-ray photoelectron spectroscopy

XPS analysis was performed to investigate the surface elemental composition and chemical state of 3DOM Ag/TiO_2 , the results shown in Fig. 3. There were mainly four types of elements including C, Ag, Ti, and O on the composite surface, as shown in Fig. 3a. Wherein, C element

Table 1

Unit cell parameters and surface area (S_{BET}), average pore size (D), pore volume (V_{total}), bandgap energy (E_g) and grain size (D^*) of TiO_2 , Ag/TiO_2 and 3DOM Ag/TiO_2

Sample	Crystal parameters		S_{BET} ($\text{m}^2 \text{g}^{-1}$)	D (nm)	V_{total} ($\text{cm}^3 \text{g}^{-1}$)	E_g (eV)	D^* (nm)
	a (Å)	c (Å)					
TiO_2	3.785	9.513	–	–	–	3.20	12.5
Ag/TiO_2	3.785	9.513	22.03	16.53	0.103	2.78	12.1
3DOM Ag/TiO_2	3.785	9.513	55.07	29.50	0.406	2.71	12.4

D^* – Average crystallite sizes of samples were calculated from Scherrer equation.

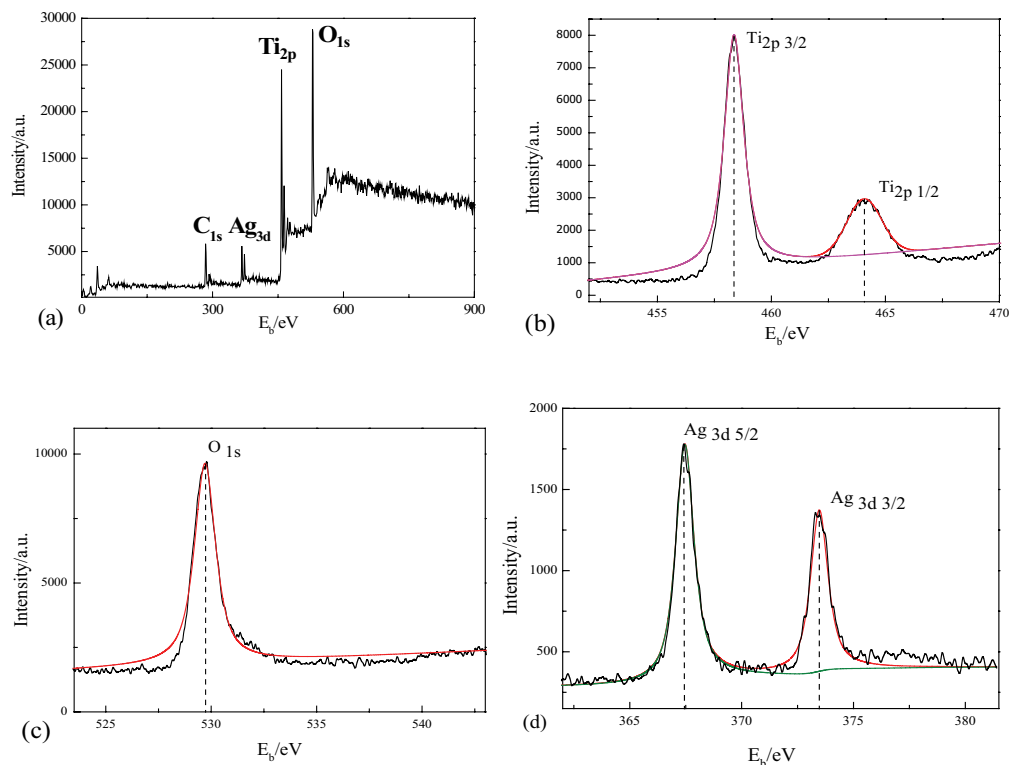


Fig. 3. XPS spectra of 3DOM Ag/TiO_2 (a), Ti 2p (b), O 1s (c), and Ag 3d (d).

may be entirely due to the PS colloidal spheres unfired or some hydrocarbon-induced brought from the instrument itself [16]. The characteristic peaks in Fig. 3b–d were attributed to Ti, O, and Ag elements. Ti element was presented in the +4 valence state, and the electronic binding energies of Ti 2p_{1/2} and Ti 2p_{3/2} were located at 464.07 and 458.33 eV, respectively. In addition, the binding energy difference is ca. 5.6 eV corresponded to the spin-orbit coupling, consistent with the literature [17]. Fig. 3c shows that the binding energies of Ag 3d_{5/2} and Ag 3d_{3/2} of 3DOM Ag/TiO_2 were 368.2 and 374.2 eV, respectively, and the energy spacing of two lines was 6.0 eV, which was the characteristic peaks of Ag metal, indicating that the Ag in the product existed in the form of Ag⁰ [16–19]. The electron binding energy of O1s was 529.73 eV attributed to the form of –2 presence of lattice oxygen, indicating that Ti–O–Ti bond was presenting in the composite material [17,20].

3.3. UV-Vis diffuse reflectance spectroscopy

In order to investigate the optical absorption of 3DOM Ag/TiO_2 composite, UV-visible diffuse reflectance spectroscopy was used, the results are shown in Fig. 4 and Table 1. Fig. 4a shows that the characteristic absorption bands of pure anatase TiO_2 appeared in the <400 nm range, consistent with the literature [19]. The absorption bands of as-synthesized 3DOM Ag/TiO_2 and Ag/TiO_2 appeared in the same area, indicating that the presence of absorption peaks was corresponding to anatase TiO_2 in the sample. Meanwhile, as-composites were produced strong absorption in the visible region, suggesting the silver dispersed relatively uniformly in TiO_2 (in agreement with the XRD results). But at the same time, we also found that the composite 3DOM Ag/TiO_2 had a blue-shift phenomenon, which might be due to the quantum size effect of 3DOM [21]. Fig. 4b is the Kubelka–Munk plot, it is not difficult to

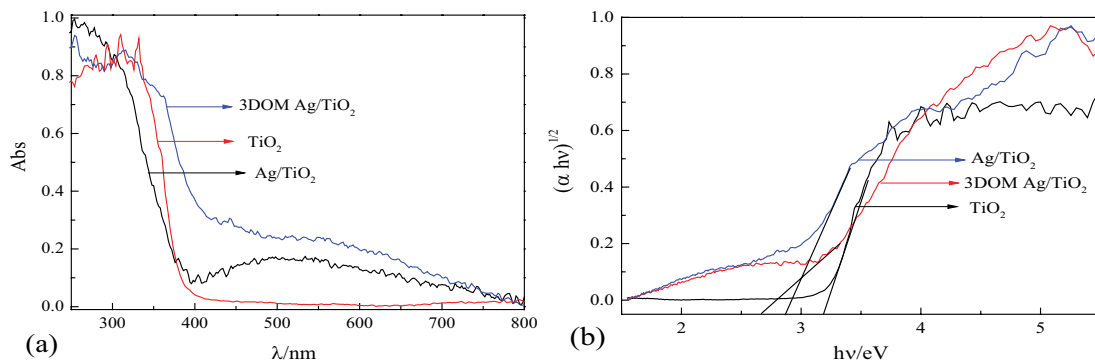


Fig. 4. UV-Visible diffuse reflectance spectra (a), Kubelka–Munk energy curve plot of TiO_2 , Ag/TiO_2 and 3DOM Ag/TiO_2 (b).

find that, compared with TiO_2 , the bandgap energy values (E_g) of Ag/TiO_2 and 3DOM Ag/TiO_2 are narrower (seen in Table 1), suggesting that Ag/TiO_2 and 3DOM Ag/TiO_2 can produce more effective photogenerated charge carrier, thus the photocatalytic activities of as-samples will be improved.

3.4. Scanning electron microscopy

In order to examine the microstructure of 3DOM Ag/TiO_2 , we conducted the SEM analysis, the result is shown in Fig. 5. From Fig. 5a and b it can be seen that the synthesized PS colloidal spheres packed closely and exhibited the hexagonal shape, and this is can be attributed to

the self-assembly process of PS colloidal spheres. In addition, as can be seen in Fig. 5a, the PS template was packed closely in multi-layers at the fault region. Fig. 5c and d is the SEM photographs of 3DOM Ag/TiO_2 composite, presenting the composite material had three-dimensionally ordered macroporous structure, which was neat and orderly, and the pore and pore were linked closely with the presence of three small-holes at the bottom of each large pore, which can attribute to the PS templates were stacked as face-centered cubic, each void exhibiting “snowflake” structure, attributed to closely packed PS colloidal spheres.

In summary, the macroporous composite has a uniform size (ca. 290 nm). The open and transparent multi-layered

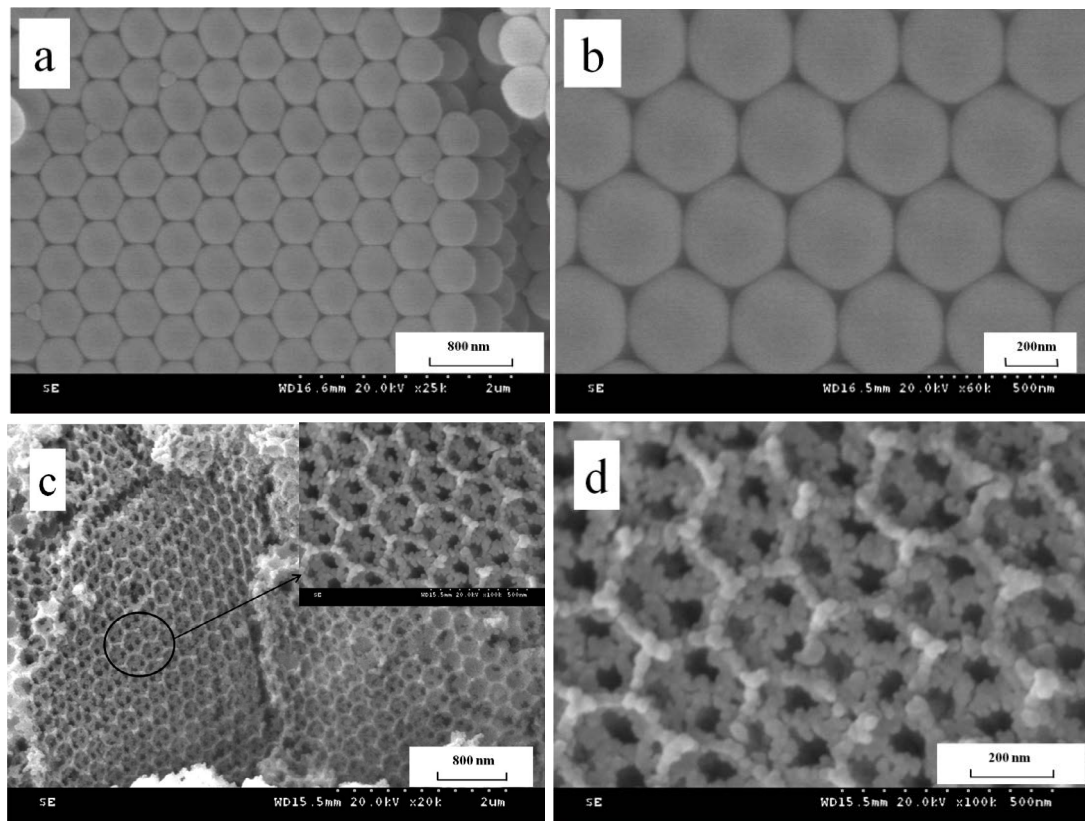


Fig. 5. SEM images of PS and 3DOM Ag/TiO_2 composite.

pore structure is beneficial to the transporting of the reactant molecules in the reaction.

3.5. Nitrogen adsorption–desorption analysis

In order to study the surface physicochemical properties of as-synthesized composites, N_2 adsorption–desorption measurement was taken, as shown in Fig. 6. According to the IUPAC nomenclature, the N_2 adsorption–desorption of 3DOM Ag/TiO₂ and Ag/TiO₂ in Fig. 6 reveal the type IV pattern curve, representing the existence of the mesoporous structure, which can be attributed to the particle accumulation on the hole-wall of 3DOM Ag/TiO₂ composite and the action of mesoporous template P123, and mesoporous of Ag/TiO₂ should be attributed to agglomeration of the particles. At the same time, as-synthesized composites had H2 hysteresis loop related to the mesoporous capillary condensation phenomenon. Additionally, the BET-specific surface area and pore volume of the two composites can be seen in Table 1. From the data in Table 1, we can find that the BET value and the pore volume of 3DOM Ag/TiO₂ are higher than that of Ag/TiO₂, and the adsorption–desorption isotherm has moved up significantly, attributed to the open macroporous structure and the “snowflake” pores of 3DOM Ag/TiO₂, indicating that the photocatalytic activity of the composite 3DOM Ag/TiO₂ is expected to be significantly improved to a certain extent [22].

3.6. Photocatalytic performance

In order to investigate the multi-mode photocatalytic activity of 3DOM Ag/TiO₂ composite, photocatalytic degradation experiments including the conditions of UV, visible and simulated sunlight were carried out, the results shown in Fig. 7. As seen in Fig. 7a, under UV light conditions, the activity of 3DOM Ag/TiO₂ in photocatalytic degradation of Malachite green was significantly higher than in other systems. Fig. 7a shows that under UV light irradiation, Malachite green gradually degraded under the effect of 3DOM Ag/TiO₂ as time going on, and almost turned colorless after 60 min. Fig. 7b shows the kinetics results of different catalysts degradation Malachite green under UV light, and 3DOM Ag/TiO₂ and Ag/TiO₂ were found not following the pseudo-first-order reaction kinetics, which wasn't inconsistent with the literature [23]; after re-fitting, we found that $1/C_t$ presented a linear relationship with reaction time t of 3DOM Ag/TiO₂ and Ag/TiO₂, meaning that the degradation Malachite green of as-composite material basic followed pseudo-second-order kinetic result. And it can be found that the degradation rate of 3DOM Ag/TiO₂ was about two times that of TiO₂.

In order to investigate 3DOM Ag/TiO₂ degradation other organic pollutants, the photocatalytic analysis of different structural dyes (CR, CV, MB) and salicylic acid (SA) was carried out under UV light in this paper, these results are shown in Fig. 7c, which expressed that the synthesized 3DOM Ag/TiO₂ had a certain effect on the degradation of various organic pollutants. In addition, in order to examine the practical application ability of 3DOM Ag/TiO₂, we also carried on the test under visible light and simulated sunlight, results are shown in Fig. 7d. As shown

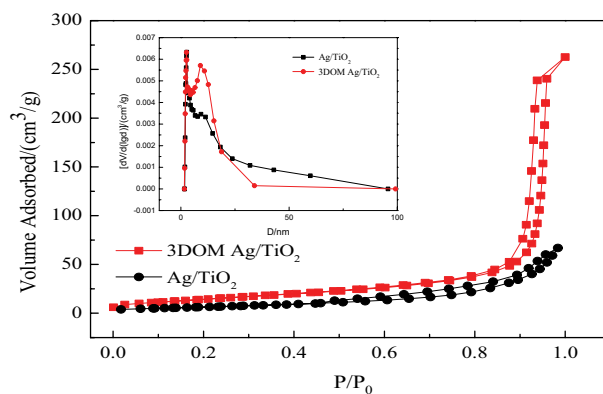


Fig. 6. N_2 adsorption–desorption isotherms and pore size distribution curves of 3DOM Ag/TiO₂ and Ag/TiO₂ (illustration is the pore size distribution curves of 3DOM Ag/TiO₂ and Ag/TiO₂).

in Fig. 7d, under visible light and simulated sunlight (illustration) catalytic conditions, although the degradation effects of 3DOM Ag/TiO₂ had not as good as that under UV condition, compared with the other catalysts, 3DOM Ag/TiO₂ still presented the highest photocatalytic activity. These results indicated that 3DOM Ag/TiO₂ had significant photocatalytic activity under multi-mode conditions. The result of the 3DOM Ag/TiO₂ photocatalytic degradation cycle experiment on MG under UV light is shown in Fig. 7e.

In order to investigate the stability of the catalyst, cycle tests were carried out. From Fig. 7e, the photocatalytic degradation result of 3DOM Ag/TiO₂ is slightly reduced after three cycles, which may be due to the blocking of the macroporous during the photocatalytic degradation process and the reduction of active sites. In addition, by comparing the XRD results of the samples before and after the photocatalytic reaction (Fig. 7f), it is not difficult to find that after the three photocatalytic cycles, the XRD test results of the samples do not find significant changes, indicating that the photocatalytic degradation reaction has basically no effect on the crystal structure of 3DOM Ag/TiO₂.

In summary, the as-prepared 3DOM Ag/TiO₂ composite in this paper has higher photocatalytic property, which can be attributed to: (1) After introducing the noble metal Ag on the surface of TiO₂, which can generate a metal-semiconductor contact between TiO₂ and Ag, since the work function of TiO₂ ($\phi_s = 3.87$ eV) is smaller than that of Ag ($\phi_s = 4.26$ eV) [24], so its Fermi level is higher, therefore, after the light irradiation, the photogenerated electrons produced by TiO₂ are easier to migrate to the surface of the particles, and then aggregate on Ag particles. Due to Ag particles being enriching electronics, it can relatively decrease the electron concentration of TiO₂ surface, thereby inhibiting the recombination probability of the photogenerated electron-holes. (2) The synthesized 3DOM Ag/TiO₂ composite owns a higher specific surface area, which can provide more active sites in photocatalytic reaction, thereby, leading to the improvement of the photocatalytic activity. (3) The open and transparent macroporous structure of 3DOM Ag/TiO₂ composite is

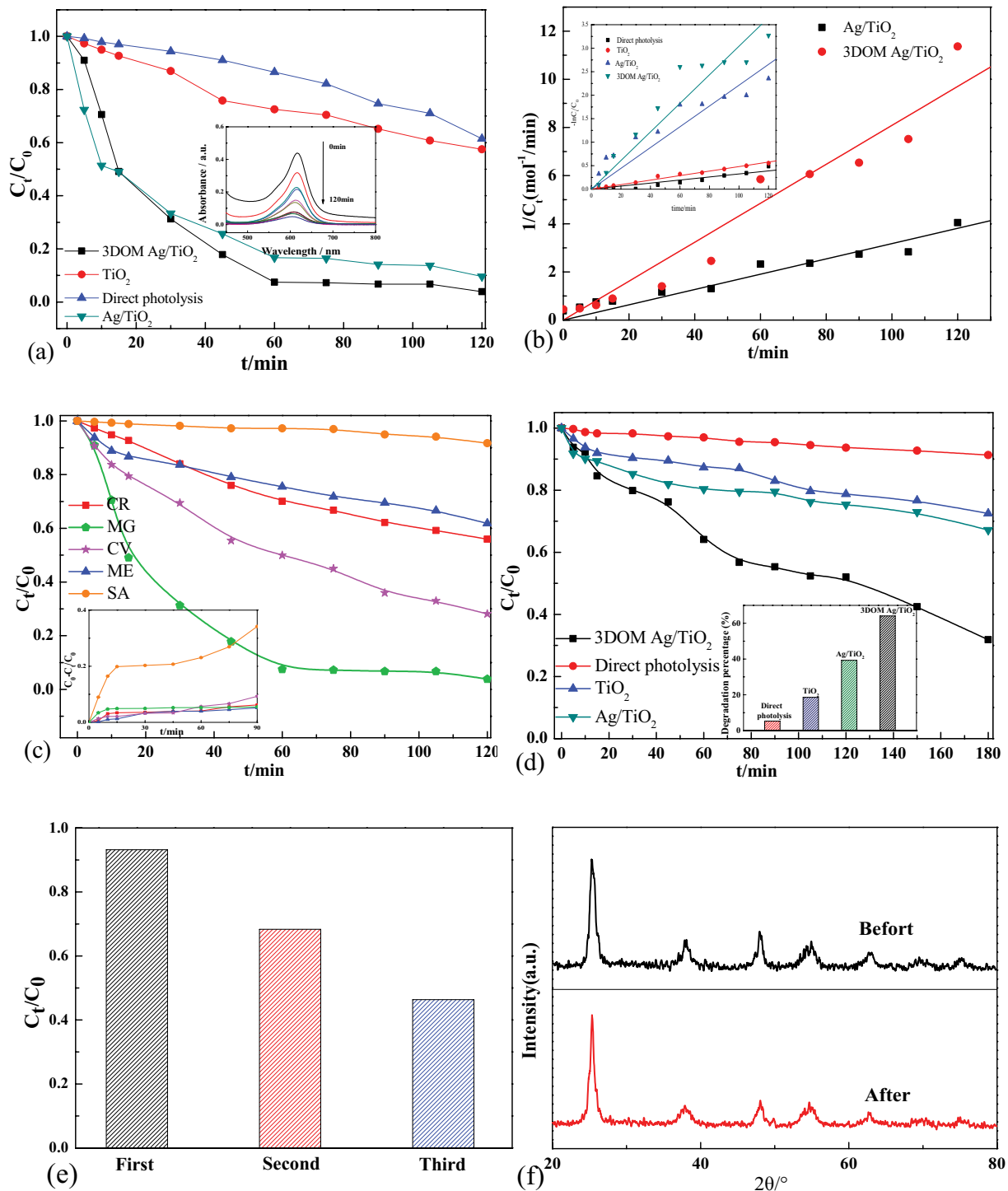


Fig. 7. (a) The results of different catalysis degradation of Malachite green under UV light (the illustration is the results of 3DOM Ag/TiO₂ degradation of Malachite green under UV light), (b) The kinetics results of different catalysis degradation of Malachite green under UV light, (c) The results of 3DOM Ag/TiO₂ degradation of different organic pollutants (CR, MG, CV, MB and SA) under UV light (illustration is the adsorption curves of different organic pollutants), (d) The results of different catalysts degradation of Malachite green under visible light (the illustration is the results of different catalysts degradation of Malachite green under simulated sunlight), (e) The cycling experiment results of 3DOM Ag/TiO₂ photocatalytic degradation of Malachite green under UV light, and (f) XRD results of 3DOM Ag/TiO₂ before and after photocatalytic degradation under UV light.

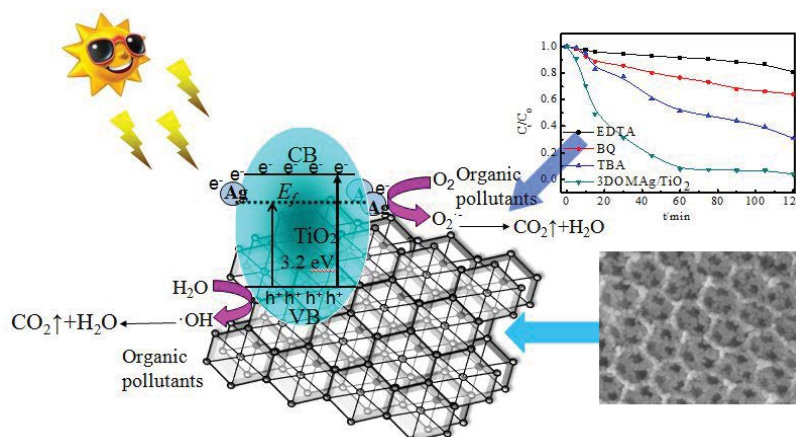


Fig. 8. Possible photocatalytic reaction mechanism of 3DOM Ag/TiO₂.

conductive to the diffusion of the reactant molecules, which can enhance the photocatalytic activity to a certain extent. (4) The strong absorption in the visible region of 3DOM Ag/TiO₂ is responsible for the higher catalytic activity in visible and simulated light conditions.

3.7. Possible photocatalytic reaction mechanism

To explore active groups in the 3DOM Ag/TiO₂ photocatalytic reaction, capture experiments were carried out in this paper. Benzoquinone (BQ), tert-butyl alcohol (TBA) and ethylene diamine tetra-acetic acid disodium salt (EDTA-2Na) were used as capture agents of superoxide radical ($\cdot\text{O}_2^-$), hydroxyl radical ($\cdot\text{OH}$) and hole (h^+), respectively, and the result are shown in Fig. 8. After adding these trapping agents, Malachite green degraded by 3DOM Ag/TiO₂ is significantly reduced, indicating that $\cdot\text{O}_2^-$, h^+ and $\cdot\text{OH}$ are the primary active species in the degradation process of Malachite green through 3DOM Ag/TiO₂. Thus, we put forward the possible photocatalytic reaction mechanism of 3DOM Ag/TiO₂, as shown in Fig. 8. When the energy of light is equal or larger than the bandgap (E_g) of 3DOM Ag/TiO₂ photocatalyst, electrons can be excited and transited to the conduction band (CB), while leaved holes in the valence band (VB). During the migrating progress of photogenerated electron–holes from the CB to the particle surface, the redox reactions between photogenerated electrons–holes and the O₂, H₂O, OH⁻ on the surface of the photocatalyst can generate active groups like $\cdot\text{OH}$ and $\cdot\text{O}_2^-$, which can degrade and mineralize organic contaminants. Meanwhile, the surface plasmon resonance (SPR) effect of silver particles can make the surface-chemical absorption red-shift to the visible region, thus enhance the photocatalytic activity in the visible region, further to improve the utilization of photocatalyst for solar energy, and ultimately achieve the purpose of the treatment of organic pollutants.

4. Conclusion

3DOM Ag/TiO₂ composite was prepared by vacuum filtration and the calcined treatment method, and a series

of studies about its structure and photocatalytic properties were carried out. Due to the SPR effect of Ag particles, the absorption of the synthesized composite can be extended to the visible region. Meanwhile, under the function of the PS colloidal crystal template, the composite presents neat and orderly pores together with an open and transparent macroporous structure. In addition, compared with Ag/TiO₂, it also has a higher specific surface area and lower bandgap energy value. In multi-modes photocatalytic experiments, 3DOM Ag/TiO₂ exhibits high photocatalytic activity, and has good degradation effect on organic pollutants with different structures under ultraviolet light irradiation, meaning 3DOM Ag/TiO₂ composite will possess a certain widespread practical application.

Acknowledgments

This study was supported by the National Natural Science Foundation of China (21376126), the Fundamental Research Funds in Heilongjiang Provincial Universities, China (135209105).

References

- [1] Y.F. Chen, W.X. Huang, D.L. He, Y.S. Tu, H. Huang, Construction of heterostructured g-C₃N₄/Ag/TiO₂ microspheres with enhanced photocatalysis performance under visible-light irradiation, *ACS Appl. Mater. Interfaces*, 16 (2014) 14405–14414.
- [2] J.Q. Jiao, Y.C. Wei, Z. Zhao, W.J. Zhong, J. Liu, J.M. Li, A.J. Duan, G.Y. Jiang, Photocatalysts of 3D ordered macroporous TiO₂-supported CeO₂ nanolayers: design, preparation, and their catalytic performances for the reduction of CO₂ with H₂O under simulated solar irradiation, *Ind. Eng. Chem. Res.*, 44 (2014) 17345–17354.
- [3] W. Qiu, C.J. Re, M.C. Gong, Y.Z. Hou, Y.Q. Chen, Structure, surface properties and photocatalytic activity of TiO₂ and TiO₂/SiO₂ catalysts prepared at different pH values, *Acta Phys. Chim. Sin.*, 27 (2011) 1487–1492.
- [4] X.H. Zhai, H.J. Long, J.Z. Dong, Y.A. Cao, Doping mechanism of N-TiO₂/ZnO composite nanotube arrays and their photocatalytic activity, *Acta Phys. Chim. Sin.*, 26 (2010) 663–668.
- [5] A.C. Li, G.H. Li, Y. Zheng, L.L. Feng, Y.J. Zheng, Photocatalytic property and reaction mechanism of (Ni-Mo)/TiO₂ nano thin

- film evaluated with Congo red, *Acta Phys. Chim. Sin.*, 28 (2012) 457–464.
- [6] N. Yan, Z. Zhao, Y. Li, Q.W. Chen, Synthesis of novel two-phase Co@SiO₂ nanorattles with high catalytic activity, *Inorg. Chem.*, 53 (2014) 9073–9079.
- [7] G. He, G. Popov, L.F. Nazar, Hydrothermal synthesis and electrochemical properties of Li₂CoSiO₄/C nanospheres, *Chem. Mater.*, 25 (2013) 1024–1031.
- [8] L. Wang, P.X. Jin, S.H. Duan, H.D. She, J.W. Huang, Q.Z. Wang, In-situ incorporation of Copper(II) porphyrin functionalized zirconium MOF and TiO₂ for efficient photocatalytic CO₂ reduction, *Sci. Bull.*, 64 (2019) 926–933.
- [9] X. Ma, K.Y. Chen, B. Niu, Y. Li, L. Wang, J.W. Huang, H.D. She, Q.Z. Wang, Preparation of BiOCl_{0.9}I_{0.1}/β-Bi₂O₃ composite for degradation of tetracycline hydrochloride under simulated sunlight, *Chin. J. Catal.*, 41 (2020) 1535–1543.
- [10] S.G. Rudisill, Z.Y. Wang, A. Stein, Maintaining the structure of templated porous materials for reactive and high-temperature applications, *Langmuir*, 28 (2012) 1024–1031.
- [11] L. Li, X.D. Huang, T.Y. Hu, J.X. Wang, W.Z. Zhang, J.Q. Zhang, Synthesis of three-dimensionally ordered macroporous composite Ag/Bi₂O₃-TiO₂ by dual templates and its photocatalytic activities for degradation of organic pollutants under multiple modes, *New J. Chem.*, 38 (2014) 5293–5302.
- [12] B.T. Holland, C.F. Blanford, T. Do, A. Stein, Synthesis of highly ordered three-dimensional, macroporous structures of amorphous or crystalline inorganic oxides, phosphates, and hybrid composites, *Chem. Mater.*, 11 (1999) 795–805.
- [13] C. Dionigi, P. Nozar, D.D. Domenico, G. Caestani, A simple geometrical model for emulsifier free polymer colloid formation, *J. Colloid Interface Sci.*, 275 (2004) 445–449.
- [14] L. Lu, L. Li, T.Y. Hu, W.Z. Zhang, X.D. Huang, J.Q. Zhang, X.J. Liu, Preparation, characterization, and photocatalytic activity of three-dimensionally ordered macroporous hybrid monosubstituted polyoxometalate K₃[Co(H₂O)PW₁₁O₃₉] amine functionalized titanium catalysts, *J. Mol. Catal. A: Chem.*, 11 (2014) 283–294.
- [15] K. Cheng, W.B. Sun, H.Y. Jiang, J.J. Liu, J. Lin, Sonochemical deposition of Au nanoparticles on different facets-dominated anatase TiO₂ single crystals and resulting photocatalytic performance, *J. Phys. Chem. C*, 117 (2013) 14600–14607.
- [16] Y.F. Gao, Y. Masuda, H. Ohta, K. Koumoto, Room-temperature preparation of ZrO₂ precursor thin film in an aqueous peroxozirconium-complex solution, *Chem. Mater.*, 16 (2004) 2615–2622.
- [17] T.G. Deepak, D. Subash, G.S. Anjusree, K.R. Narendra Pai, S.V. Nair, A.S. Nair, Photovoltaic property of anatase TiO₂ 3D mesoflowers, *ACS Sustainable Chem. Eng.*, 2 (2014) 2722–2780.
- [18] C.D. Gu, C. Cheng, H.Y. Huang, T.L. Wong, N. Wang, T.Y. Zhang, Growth and photocatalytic activity of dendrite-like ZnO@Ag heterostructure nanocrystals, *Cryst. Growth Des.*, 9 (2009) 3278–3285.
- [19] J. Liu, Y.J. Hu, F. Gu, C.Z. Li, Flame synthesis of ball-in-shell structured TiO₂ nanospheres, *Ind. Eng. Chem. Res.*, 48 (2009) 735–739.
- [20] L.Q. Jing, B.F. Xin, L.F. Yuan, L.P. Xue, B.Q. Wang, H.G. Fu, Effects of surface oxygen vacancies on photophysical photochemical processes of Zn-doped TiO₂ nanoparticles and their relationships, *J. Phys. Chem. B*, 110 (2006) 17860–17865.
- [21] M. Anpo, T. Shima, S. Kodama, Y. Kubokawa, Photocatalytic hydrogenation of CH₃CCH with H₂O on small-particle TiO₂: size quantization effect and reaction intermediates, *J. Phys. Chem.*, 91 (1987) 4305–4310.
- [22] L. Li, X.D. Huang, J.Q. Zhang, W.Z. Zhang, F.M. Ma, Z.X. Xiao, S. Gai, D.D. Wang, N. Li, Multi-layer three-dimensionally ordered bismuth trioxide/titanium dioxide nanocomposite: synthesis and enhanced photocatalytic activity, *J. Colloid Interface Sci.*, 4 (2015) 13–22.
- [23] Y. Yang, G.Z. Wang, Q. Deng, DHL. Ng, H.J. Zhao, Microwave-assisted fabrication of nanoparticulate TiO₂ microspheres for synergistic photocatalytic removal of Cr(VI) and methyl orange., *ACS Appl. Mater. Interfaces*, 6 (2014) 3008–3015.
- [24] Y. Komuro, Y. Matsumoto, Electron beam irradiation-induced reduction of SnO₂ deposited on TiO₂(110) surfaces, *J. Phys. Chem. C*, 115 (2011) 6618–6621.